Journal of Engineering Science | Vol. XXXII, no. 1 (2025), pp. 7 - 17
Fascicle Industrial Engineering | ISSN 2587-3474
Topic Electrical Engineering and Power Electronics | eISSN 2587-3482

https://doi.org/10.52326/jes.utm.2025.32(1).01
UDC 621.314.57

LINEAR AND NON-LINEAR VOLTAGE-TO-FREQUENCY MULTI-ZONE CONTROL OF SYNCHRONOUSLY MODULATED POWER ELECTRONIC INVERTERS

Valentin Oleschuk*, ORCID: 0000-0002-7413-4867,
Irina Vasiliev, ORCID: 0000-0003-3996-6745

Institute of Power Engineering of Technical University of Moldova, 5 Academy Str., Chisinau, Republic of Moldova
* Corresponding author: Valentin Oleschuk, *oleschukv@hotmail.com*

Received: 12. 14. 2025
Accepted: 01. 28. 2025

Abstract. The publication presents a brief analysis of the results from the study on power electronic converters based on voltage source inverters (VSIs) and neutral-point-clamped inverters (NPCIs) with scalar control modes implemented by algorithms of synchronous multi-zone pulsewidth modulation (SMZ PWM). This control and modulation strategy can provide both linear and required non-linear relationships between the output voltage and the fundamental frequency of the inverters (Voltage/Frequency (V/F)). The simulation results demonstrated the behavior of two inverter-based drive systems controlled by algorithms of SMZ PWM, providing both linear and non-linear V/F relationships. Thus, the appropriately modified techniques of SMZ PWM, used for regulating inverters of adjustable speed electric drives, ensure continuous synchronization and symmetry of phase and line voltages in these electrical power conversion systems over the entire regulation range.

Keywords: *pulsewidth modulation, variable-voltage variable-frequency drive, voltage source inverter, voltage spectrum.*

Abstract. Publicația prezintă o scurtă analiză a rezultatelor studiului convertoarelor electronice de putere bazate pe invertoare cu sursă de tensiune și invertoare cu fixare în punct neutru cu moduri de control scalar implementate prin algoritmi de modulație sincronă a lățimii de impuls multi-zonă. Această strategie de control și modulare poate oferi atât relații liniare, cât și neliniare necesare între tensiunea de ieșire și frecvența fundamentală a invertoarelor. Rezultatele simulării au demonstrat comportamentul a două sisteme de acționări bazate pe invertor controlate de algoritmi de modulației multi-zonă sincronă, oferind atât relații liniare, cât şi neliniare între tensiunea de ieșire a invertoarelor şi frecvența fundamentală. Astfel, tehnicile de modulație multi-zonă sincronă modificate corespunzător, utilizate pentru reglarea invertoarelor de acționări electrice cu viteză reglabilă, asigură sincronizarea și simetria continuă a tensiunilor de fază și linie în aceste sisteme de conversie a energiei electrice pe întregul domeniu de reglare.

Cuvinte cheie: *invertor sursă de tensiune, modulație de lățime a impulsurilor, acționări electrice reglabile, spectru de tensiune.*

1. Introduction

Power electronic converters of electrical energy parameters based on power transistors are widely used installations in modern electrical and energy systems [1].

One of the most important areas of application of inverter-based power conversion systems are variable-frequency electric drives with asynchronous electric motors [2−3]. It is known that the control modes of inverters of variable frequency drives in many cases are carried out according to the linear law of constancy of the ratio of the output voltage of the converter to the fundamental frequency of the system (*Voltage/Frequency* = *const* or *V/F* = *const*) [4-9]. Therefore, these control modes can be implemented using control boards based on dSpace [5], using systems controlled by space-vector pulse-width modulation (PWM) algorithms for determining pulse patterns of control signals [7]. Also, these modes can be implemented using control and regulation systems based on programmable logic arrays (FPGAs) [8], as well as control systems with optimally tuned PI controllers [9]. Figure 1 shows the corresponding diagram showing the linear *V/F* relationship between the nominal output voltage of the inverter and its operating frequency [4].

It is also known that for some specialized frequency-controlled electric drives with specific operating conditions, more efficient regulation of systems can be ensured by scalar control modes with non-linear Voltage-to-Frequency adjustment (with nonlinear *V/F* regulation modes) [10-11].

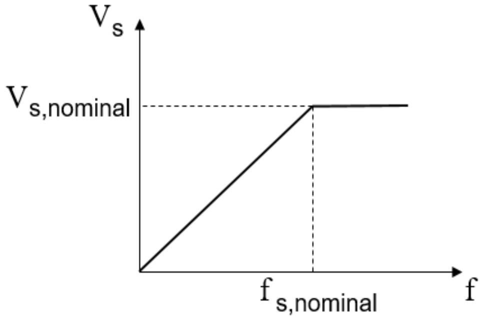

Figure 1. *V/F* linear regulation during scalar control regime of VSI [4].

At the same time, for power conversion systems based on inverters with increased power levels, it is necessary to ensure the symmetry of the output voltage waveform of the drive inverters in order to eliminate unwanted sub-harmonics (of the fundamental frequency) from the output voltage and current spectra of the inverters [12].

Thus, for continuous synchronization of voltage in PWM inverters of drive systems, as well as for providing improved harmonic composition of output voltage, specialized PWM methods and techniques were investigated [13-25]. These methods and techniques were based both on the standard space-vector approach to determining the pulse sequences of inverter control signals [13,15,17,19,21-23,25], and on a new multi-zone control strategy for modulated inverters (based on the method of synchronous multi-zone pulse-width modulation (SMZ PWM)) [14,16,18,20,24]. In particular, the developed methods and techniques of synchronous modulation have found application for controlling three-phase [13], five-phase and split-phase [14] PWM inverters of motor drives, Also, the developed algorithms of synchronous PWM have found application for controlling medium-power inverters with low switching frequency [15], six-phase inverters of vehicle drives [16], three-level inverters [17], and drive systems based on quadruple inverters [18].

In addition, in terms of high-power motor drive systems, the corresponding synchronous PWM methods and techniques have been widely used to control traction inverters [19], fixed-neutral-point power inverters [20], as well as medium-voltage inverters [21]. Also, methods of synchronous PWM have been used to control dual inverters of electric vehicles [22], inverters with vector control modes [23], multi-inverter drive systems [24], and power inverters for traction motor drives [25].

It is necessary to mention, that not only linear *V/F* control modes have been analyzed in the mentioned above papers, but also some non-linear control regimes of inverter-based system have been investigated in [18].

Accordingly, this paper presents the results of a study of two promising topologies of variable frequency electric drives: split-phase motor drive based on six-phase voltage source inverter (VSI), and dual neutral-point-clamped inverters (NPCIs) of drive system with two stator windings of induction motor. Both these topologies are regulated by a modernized scheme of SMZ PWM that assures continuous voltage synchronization and both linear and non-linear *V/F* control relationships over the entire adjustment range.

2. Linear *V/F* control of VSI with SMZ PWM

Figure 2 shows structure a three-phase VSI feeding the corresponding induction machine IM. Voltage space vectors (six switching vectors 1 - 6 and two zero vectors 0 and 7) are also shown in Figure 2 [24].

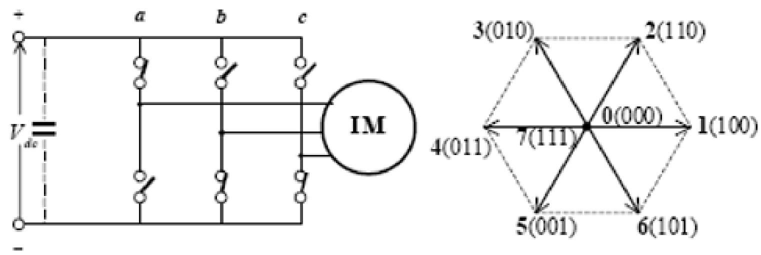

Figure 2. Structure of three-phase VSI feeding asynchronous induction motor IM, and voltage space vectors of three-phase inverter.

Figure 3 shows (inside the 60^0 clock-cycle) diagrams of sequence of switchings, and the pole and line voltages of modulated VSI adjusted by algorithm of continuous SMZ PWM, insuring synchronization and symmetry of the output voltage of VSI for scalar control mode of system [24].

The principle of voltage synchronization in a three-phase VSI is based on continuous synchronization of the positions of the central control signals at the centers of 60-degree clock intervals. Simultaneously, symmetrical formation of the remaining control signals around the corresponding central signal has to be provided.

The scheme of SMZ PWM includes a step-by-step determination of the boundary frequencies F_i and F_{i-1} as a function of the duration of clock subintervals τ, which are transition frequencies between control sub-ranges [24]. Figure 4 presents a generalized diagram for determining the parameters (durations and temporary position) of control signals (control pulses, see Figure 3) of VSI regulated by SMZ PWM in relation to scalar *V/F = const* operating mode [24].

As it follows from the generalized diagram for determining the parameters of control signals of a three-phase VSI shown in Figure 4, one of the main control signals of the scheme of SMZ PWM is the central signal β_1 in the middle of the 60-degree clock intervals (see Figure 3), determined as a function of the modulation coefficient *m* of VSI as $\beta_1 = 1.1m\tau$ for the scalar control regime of the system according to the law of constancy of the ratio of voltage to frequency (*V/F = const*) [24].

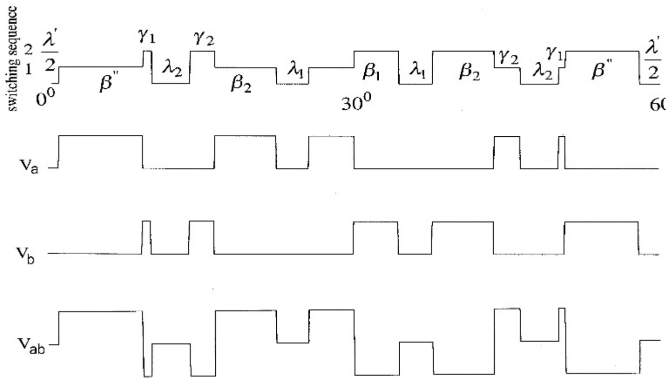

Figure 3. Switching sequence of VSI regulated by SMZ PWM, and pole and line voltages V_a, V_b, and V_{ab} inside the 60^0 clock interval.

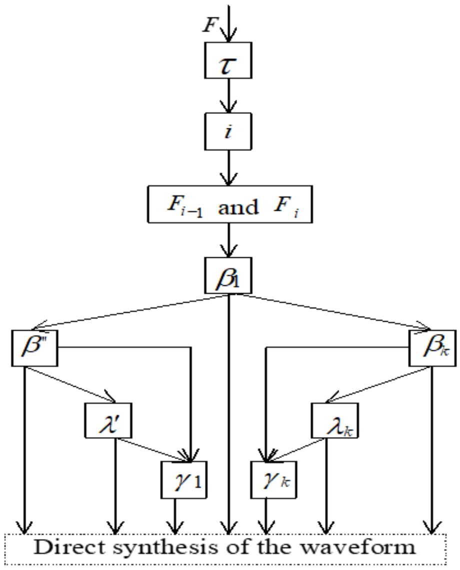

Figure 4. Generalized diagram for determining the parameters of control pulses of VSI adjusted by SMZ PWM.

As an illustration of operation of three-phase VSI PWM during *V/F = const* control regime, Figures 5 and 6 present waveforms of the pole voltages V_a, V_b, V_c, and line voltage V_{ab} of VSI with algorithms of continuous (Figure 5) and discontinuous (Figure 6) SMZ PWM.

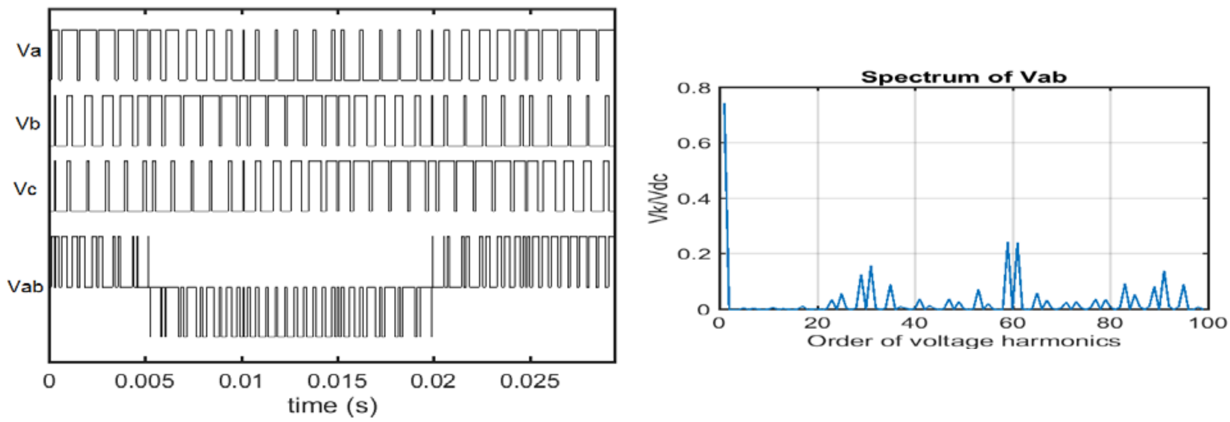

a) b)

Figure 5. Voltage waveforms of VSI with continuous SMZ PWM (a), and spectrum of the line voltage V_{ab} (b) ($F = 35.0$ Hz, $m = 0.70$, $F_s = 1.00$ kHz).

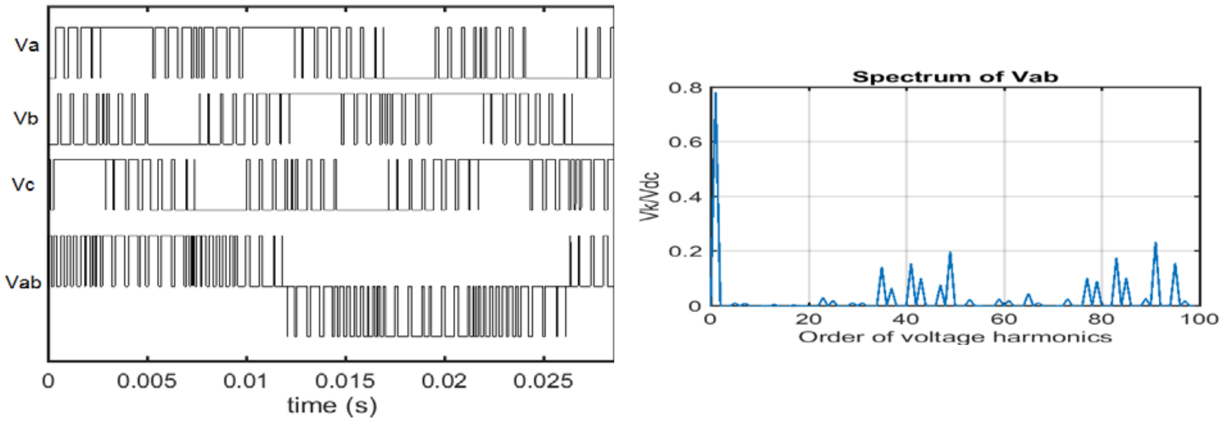

a) b)

Figure 6. Voltage waveforms of VSI with discontinuous SMZ PWM (a), and spectrum of the line voltage V_{ab} (b) ($F = 35.0$ Hz, $m = 0.70$, $F_s = 1.00$ kHz).

3. Non-linear Voltage-to-Frequency control of VSI-based drive installations

As shown in [18], a specialized nonlinear change of value of the β_1-signal as a function of the modulation coefficient *m* of VSIs makes it possible to provide various nonlinear relationships between the magnitude of the output voltage of VSIs and the fundamental frequency of system during the regulation process. Such nonlinear laws and algorithms for controlling converter systems for variable-frequency electric drives make it possible to ensure the effective operation of specialized adjustable speed ac drives with specific loads and special control modes [10-11].

In particular, Table I shows the basic control parameters for three examples of control modes of drive systems, including the standard scalar linear control mode $V/F = const$, as well as two non-standard (non-linear) control modes $V^2/F = const$ and $V^{3/2}/F = const$ [18]. The last two modes are characterized by nonlinear relationships between voltage and frequency and can be used to control asynchronous electric drives with some special types of loads [11]. Table I also includes the corresponding relative values of the two overmodulation threshold frequencies F_{ov1} and F_{ov2} [18], which are important parameters of the control strategy in the overmodulation control zone of inverters.

Table 1

Basic control parameters for both linear and non-linear synchronous regulation of VSI-based drives

Control regime	Central control signal β_1	Overmodulation frequency F_{ov1}	Overmodulation frequency F_{ov2}
$V/F=const$	$1.1m\tau$	$0.907F_m$	$0.952F_m$
$V^2/F=const$	$1.1\sqrt{m}\tau$	$0.823F_m$	$0.907F_m$
$V^{3/2}/F=const$	$1.1\sqrt[3]{m^2}\tau$	$0.866F_m$	$0.931F_m$

Note: β_1 – width of the central control signal; F_{ov1} – the first threshold overmodulation frequency; F_{ov2} – the second threshold overmodulation frequency; F_m – the maximum operating frequency; *m* – modulation index of inverter; τ – width of sub-cycle; *V* –output voltage of inverter; *F* – output frequency of inverter.

Figure 7 shows the dependence of the normalized output voltage of a three-phase VSI on the operating frequency (at the maximum operating frequency of the system equal to $F_m = 50.0$ Hz) in relation to the three above-mentioned control modes presented in Table 1 [18]. In this case, it is also possible to implement various numerous intermediate control regimes, characterized by other functional dependencies for determining the duration of the β_1-signals. As an example, dotted line in Figure 7 shows the non-linear *Voltage/Frequency* ratio of drive system in the process of regulating the fundamental frequency according to the law $V^{4/3}/F = const$ [18].

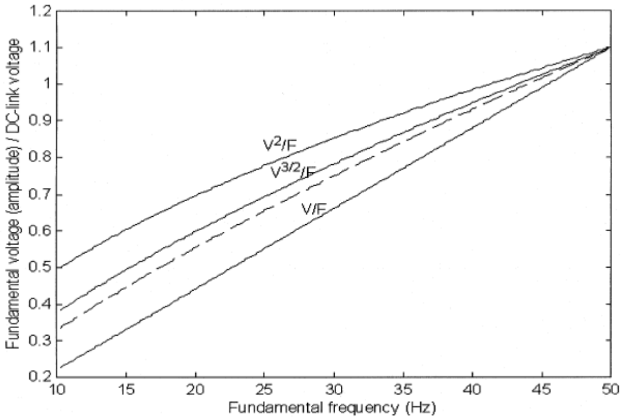

Figure 7. Non-linear and linear *Voltage-to-Frequency* control regimes.

Ones of the interesting and promising structures of drives currently are split-phase motor drives [14]. In this case, the asynchronous motor has two sets of windings, spatially shifted by 30 el. degrees with isolated neutral points N_{abc} and N_{xyz} (Figure 8 [14]). Its phase voltages V_{as} and V_{xs} are calculated using (1) – (2) [14]:

$$V_{as} = V_a - 0.333(V_a + V_b + V_c) \quad (1)$$

$$V_{xs} = V_x - 0.333(V_x + V_y + V_z), \quad (2)$$

where: $V_a, V_b, V_c, V_x, V_y, V_z$ are the corresponding voltages at poles of six-phase VSI (see Figure 8).

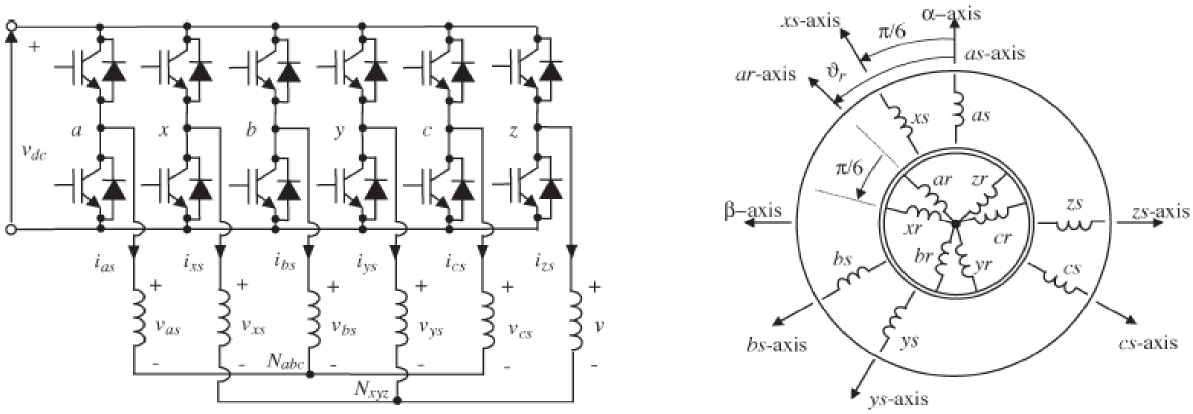

Figure 8. Split-phase electric drive with neutral points N_{abc} and N_{xyz}.

Figure 9 and Figure 10 show basic voltage waveforms of this installation, and spectral characteristics of the phase voltage in split-phase drive in a nonlinear system control mode according to the law $V^2/F = const$. The diagrams in Figure 9 show the base voltages and the phase voltage spectrogram for the system based on VSI controlled by continuous SMZ PWM (CPWM) algorithms. The diagrams in Figure 10 show the base voltages and the phase voltage spectrogram for the system with VSI controlled by discontinuous SMZ PWM algorithms with 30-degree intervals of the non-conducting state of the power switches (DPWM30). The average switching frequency of VSI and the operating frequency of split-phase drive are 1050 Hz and 34 Hz, respectively.

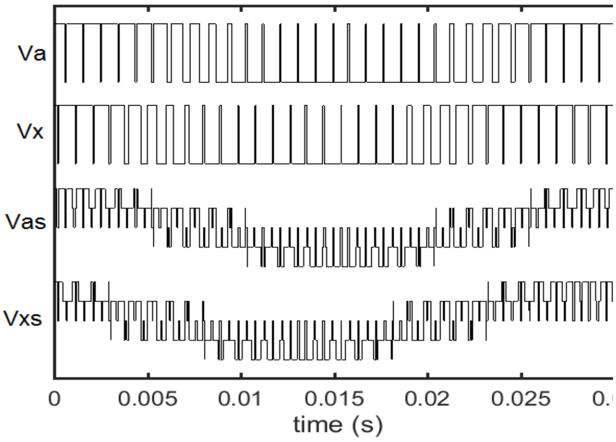

a)

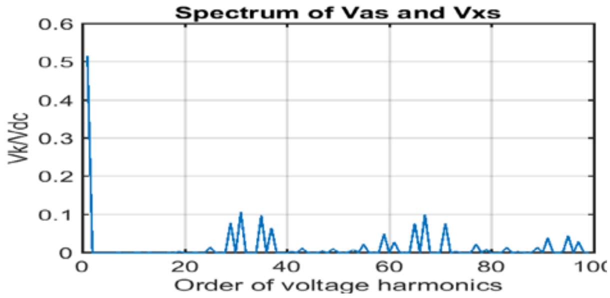

b)

Figure 9. Waveforms of the pole and phase voltages (a), and harmonic composition of the phase voltage (b) (CPWM).

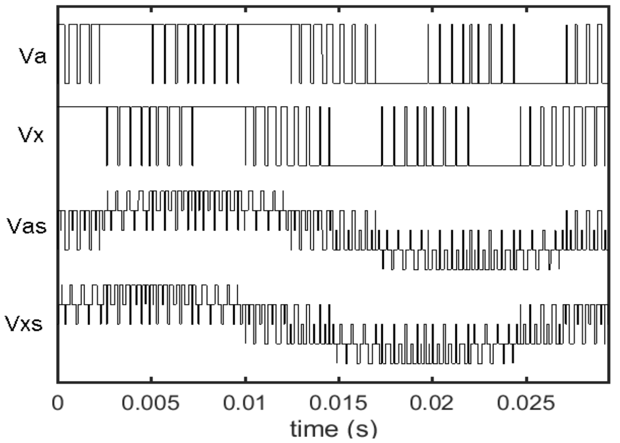

a)

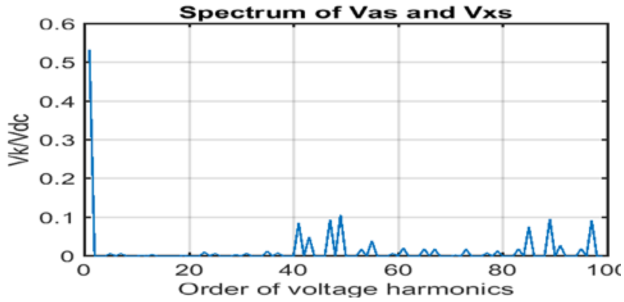

b)

Figure 10. Waveforms of the pole and phase voltages (a), and harmonic composition of the phase voltage (b) (DPWM30).

Figure 11 shows the results of calculating the Weighted Total Harmonic Distortion factor of phase voltage Vas ( ) depending on the modulation index *m* of a six-phase VSI controlled by the above-mentioned algorithms of both synchronous continuous PWM and discontinuous PWM in the $V^2/F = const$ control mode, with VSI switching frequency equal to 1050.0 Hz.

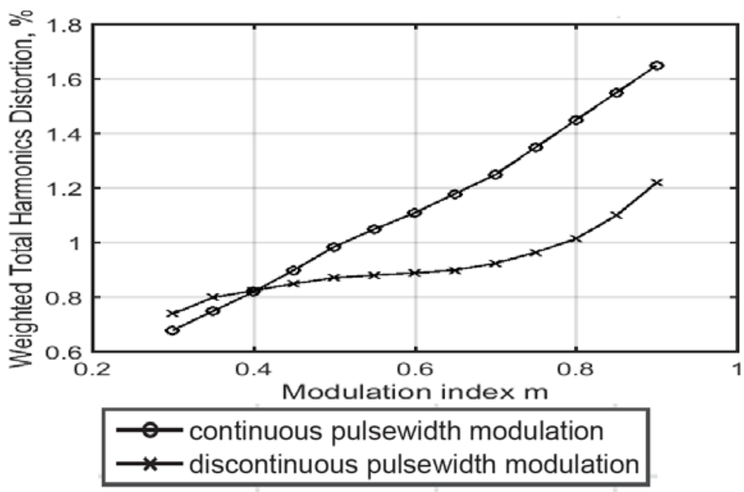

Figure 11. *WTHD* factor of the phase voltage V_{as} versus modulation index *m* of the inverter.

4. NPCI-based drive installation with two stator windings of induction motor and non-linear *V/F* control

Figure 12 shows the structure of a variable-frequency adjustable speed drive installation with two stator win-dings of an asynchronous motor, specially connected (see thick lines) to the corresponding outputs of two modulated NPC inverters NPCI1 and NPCI2 [20].

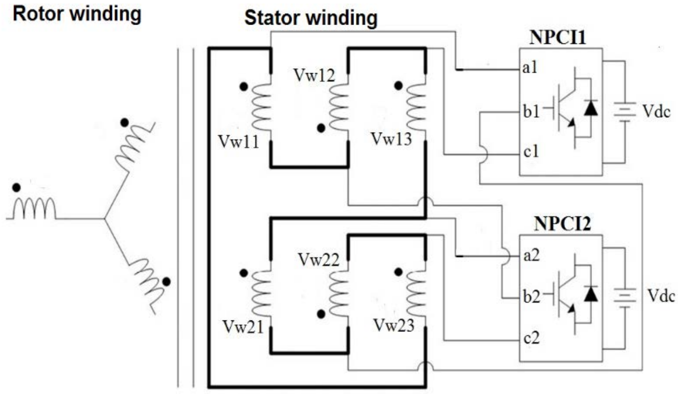

Figure 12. Topology of NPCI-based ac drive with two stator windings of electrical motor.

Instantaneous voltage values on the corresponding stator windings V_{w11} - V_{w13} and V_{w21} - V_{w23} of the electric drive (Figure 12) with specialized control scheme of NPCIs [20] are determined as functions of the corresponding pole voltages of NPCIs in accordance with (3) - (4):

$$V_{w11} = V_{a1} - V_{b2},\ \ V_{w12} = V_{b2} - V_{c1},\ \ V_{w13} = V_{c1} - V_{a2} \tag{3}$$

$$V_{w21} = V_{a2} - V_{b1},\ \ V_{w22} = V_{b1} - V_{c2},\ \ V_{w23} = V_{c2} - V_{a1} \tag{4}$$

Figures 13–14 show the main voltage waveforms and spectrograms of phase voltage in the variable frequency drive system with two stator windings of the electric motor (normalized values of pole and line voltages of the first inverter NPCI1 (V_{a1}, V_{b1} and V_{a1b1}), voltage on the stator winding of the electric motor V_{w11}, as well as the spectral composition of the voltage V_{w11}). This corresponds to the case of nonlinear regulation of NPCIs with SMZ PWM according to the control law $V^{3/2}/F = const$.

The diagrams presented in Figure 13 illustrate the process when the regulation of the NPCIs is carried out on the basis of a continuous scheme of SMZ PWM (CPWM). The diagrams presented in Figure 14 illustrate the process in the system when regulating the NPCIs is based on the algorithms of discontinuous SMZ PWM (DPWM). Features and peculiarities of both continuous and discontinuous schemes of SMZ PWM, applied for liner *V/F* control of NPCIs, are described in [20]. The operating frequency of drive installation is $F = 37\ Hz$, the switching frequency of two NPCIs is equal to 1050.0 Hz.

The presented in Figures 13-14 results show that the winding voltage V_{w11} feeding electric motor has quarter-wave symmetry, and in its spectrum there are no even harmonics and subharmonics in the analyzed mode of nonlinear *V/F* regulation of drive installation.

Figure 15 shows the calculated Weighted Total Harmonic Distortion factor of the winding voltage V_{w11} ($WTHD = (1/V_{w11_1})(\sum_{k=2}^{1000}(V_{w11_k}/k)^2)^{0.5}$) depending on the modulation index m of NPCIs for the analyzed variable frequency drives with NPCIs, regulated in accordance with continuous (CPWM) and discontinuous (DPWM) versions of SMZ PWM. In this case, the system operated in the $V^{3/2}/F = const$ control mode (**mode 1**) and in the $V^2/F = const$ control mode (**mode 2**). Switching frequency of NPCIs is equal to 1050.0 Hz. The presented data prove the fact that for the system regulated by non-linear *V/F* modes discontinuous scheme of SMZ PWM assures a better harmonic composition of the winding voltage compared to the continuous scheme of SMZ PWM, if $m = 0.60 \div 1.00$.

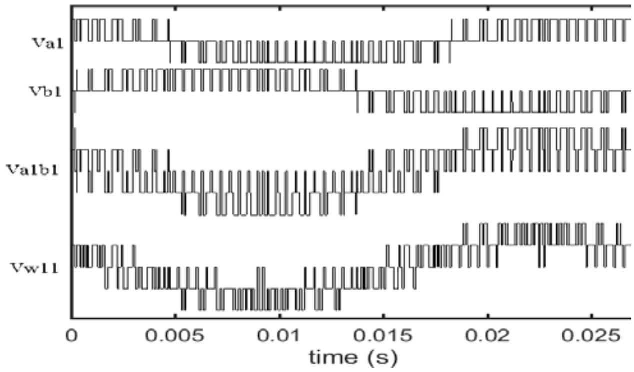

a)

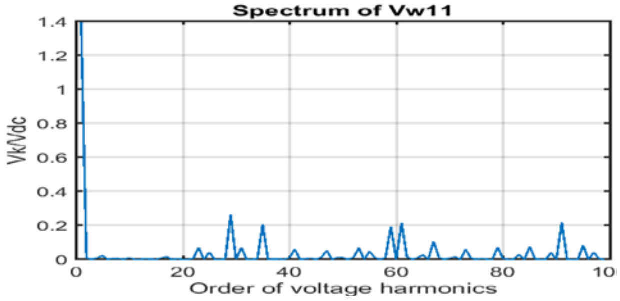

b)

Figure 13. Voltages (a), and spectrum (b) of the V_{w11} voltage (CPWM).

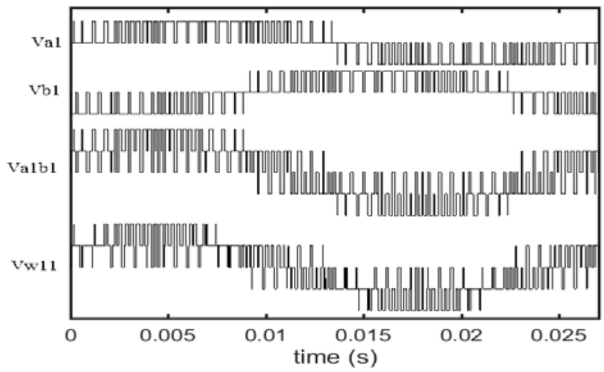

a)

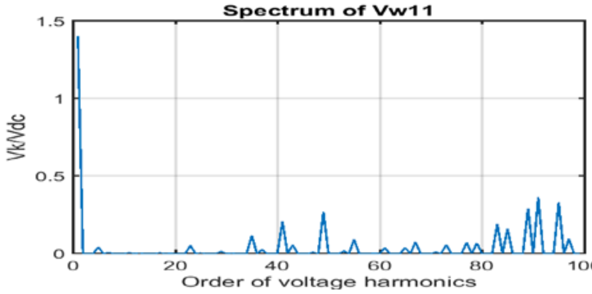

b)

Figure 14. Voltages (a), and spectrum (b) of the V_{w11} voltage (DPWM).

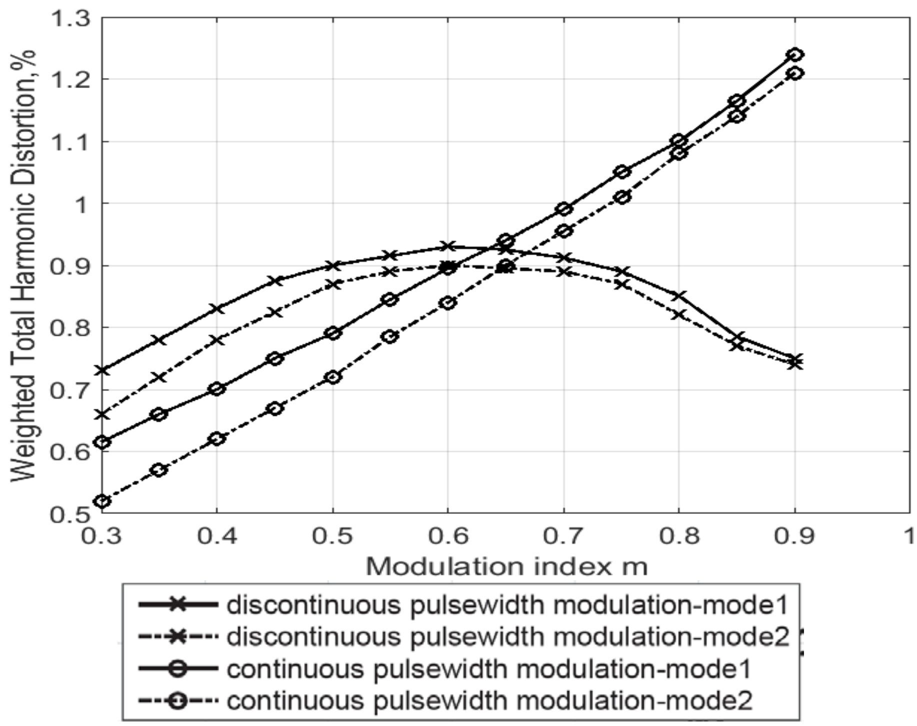

Figure 15. *WTHD* factor of the winding voltage V_{w11} versus modulation index *m* of two NPCIs adjusted by synchronous multi-zone pulsewidth modulation.

5. Conclusion

The modified scheme of SMZ PWM of VSIs and NPCIs of variable-frequency electric drives, applied for regulation of two topologies of inverter-based ac drives, makes it possible to provide control modes with the required non-linear relationships between the output voltage of inverters and the operating frequency of drive installations. In this case, the required voltage and frequency ratio is ensured by the corresponding smooth adjustment of the duration of the central (within 60-degree clock intervals) control signals of the VSIs and NPCIs, regulated by SMZ PWM.

Thus, modernized schemes and algorithms of SMZ PWM for regulation of VSI- and NPCI-based variable-frequency drives ensure continuous synchronization and symmetry of the basic voltages in apparatuses over the entire control range. The spectra of the base voltages of these installations do not contain even harmonics and subharmonics (of the operating frequency of the drive installations), which helps to reduce losses in the installations and increase their operating efficiency. And this is especially important for the medium-power and high-power adjustable speed drives.

Conflict of Interest: The authors declare no conflicts of interest.

References

1. Rodriguez, J.; Blaabjerg, F.; Kazmierkowski, M.P. Energy transition technology: The role of power electronics. *Proc. of the IEEE* 2023, 111 (4), pp. 329-334.
2. Ehsani, M.; Singh, K.V.; Bansal, H.O.; Mehrjardi, R.T. State of the art and trends in electric and hybrid electric vehicles. *Proc. of the IEEE* 2021, 109 (6), pp. 967-984.
3. Shetty, A.; Suryanarayana, K. Variable frequency and voltage control of induction motor for electric vehicles. *Advances in Renewable Energy and Electric Vehicles* 2022, pp. 449-463.
4. Pena, J.M.; Diaz, E.V. Implementation of V/f scalar control for speed regulation of a three-phase induction motor. In: *Proc. of* IEEE ANDESCON'2016, Arequipa, Peru, Oct. 2016, 6 p.
5. Tigade, C.; Sreejeth, M. Implementation of V/f adjustable speed drive for induction motor using dSPACE dS1104. In: *Proc. of IEEE Int'l Conf. on Power Electronics, Intelligent Control and Energy Systems* (ICPEICES'2018), 2018, Delhi, India, Oct. 2018, pp. 938-943.
6. Hussein, T.A. V/F control of three phase induction motor driven by VSI based on SVPWM. In: *Proc. of IEEE Int'l Conf. on Advance of Sustainable Engg. and its Appl.* (ICASEA'2021), Wasit, Iraq, Oct. 2021, pp. 49-53.
7. Waleed, U.; Waseem, M.; Shaukat, H.; Ali Ijaz, Almalaq, A.; Mohamed, M.A. An efficient FPGA based scalar V/f control mechanism of three phase induction motor for electric vehicles. In: *Proc. of IEEE Australasian Universities Power Engg. Conf.* (AUPEC'2021), Perth, Australia, Nov. 2021, 6 p.
8. Winslet, B.S.; Preethi, K.; Krishna, K.S.; Prasad, J.S.V. Performance of induction motor using V/F control technique. In: *Proc. of IEEE 2nd Mysore Sub Section Int'l Conf.* (MysuruCon'2022), Mysuru, India, Oct. 2022, 6 p.
9. Keskin, B.; Eminoglu, I. Optimally tuned PI controller design for V/f control of induction motor. In: *Proc. of Int'l Congress on Human-Computer Interaction, Optimization and Robotic Applications* (HORA'2022), Ankara, Turkey, June 2022, pp. 1-5.
10. Sruthi, M.; Nagamani, C.; Ilango, G.S, An improved algorithm for direct computation of optimal voltage and frequency for induction motors. *Engineering Science and Technology* 2017, 20 (5), pp. 1439-1445.
11. Graciola, C.L.; Goedtel, A.; Angélico, B.A.; Castoldi, M.F.; Costa, B.L.G. Energy efficiency optimization strategy for scalar control of three-phase induction motors. *Journal of Control, Automation and Electrical Systems* 2022, 33, pp. 1032–1043.
12. Mohan, N.; Undeland, T.M.; Robbins, W.P. *Power Electronics*, 3rd ed., John Wiley & Sons, Hoboken, New Jersey, USA, 2002, 832 p.
13. Beig, A.R. Constant *v/f* induction motor drive with synchronised space vector pulse width modulation. *IET Power Electron.* 2012, 5 (8), pp. 1446-1455.
14. Oleschuk, V.; Barrero, F. Standard and non-standard approaches for voltage synchronization of drive inverters with space-vector PWM: A survey. *International Review of Electrical Engineering* 2014, 9 (4), pp. 688-707.

15. Tripathi, A.; Narayanan, G. Evaluation and minimization of low-order harmonic torque in low-switching-frequency inverter fed induction motor drives. *IEEE Trans. Ind. Appl.* 2016, 52 (2), pp. 1477-1488.
16. Oleschuk, V.; Griva, G. Synchronised space-vector modulation for six-phase automotive drive with controlled switching frequency. *International Review of Electrical Engineering* 2009, 4(1), pp. 50-56.
17. Wei Chen, Haiwei Sun, Xin Gu, Changliang Xia. Synchronized space vector PWM for three level VSI with lower harmonic distortion and switching frequency. *IEEE Trans. Power Electron* 2016, 31(9), pp. 6428-6441.
18. Oleschuk, V., Sanjeevikumar, P.; Cernat, M.; Fedak, V.; Pastor, M. Multiphase quad-inverter system with feedforward synchronous PWM and nonlinear voltage regulation. In: *Proc. of IEEE Int'l Conf. on Power Electronics and Motion Control* (PEMC'2016), Varna, Bulgaria, Sept. 2016, pp. 1180-1185.
19. Xiao, L.; Li, J.; Xiong, Y.; Chen, J.; Gao, H. Strategy and implementation of harmonic-reduced synchronized SVPWM for high-power traction machine drives. *IEEE Trans. Power Electron* 2020, 35(11), pp. 12457-12471.
20. Oleschuk, V.; Vasiliev, I. Motor drive system with double-delta-sourced stator winding and two modulated NPC converters. In: *Proc. of IEEE Int'l Conf. 2020 KhPI Week on Advanced Technology,* Kharkiv, Ukraine, Oct. 2020, pp. 357-362.
21. Zhang, G.; Zhou, Z.; Shi, T.; Xia, C.L. An improved multi-mode synchronized space vector modulation strategy for high-power medium-voltage three-level inverter. *IEEE Trans. Power Electron* 2021, 36(4), pp. 4686-4696.
22. Linghao Wu, Jian Li, Yang Lu, Kun He. Strategy of synchronized SVPWM for dual three-phase machines in full modulation range. *IEEE Trans. Power Electron* 2022, 37(3), pp. 3272-3282.
23. Kumari, P.; Tripathi, A. Synchronized hybrid PWM for high power IM drives operated in vector control mode. In: *Proc. of IEEE IAS Global Conf. on Emerging Technologies* (GlobConET'2022), Arad, Romania, May 2022, pp. 999-1004.
24. Oleschuk, V.; Tirsu, M. Basic aspects of the theoretical and practical relevance of the method of synchronous multi-zone PWM for power inverters, In: *Proc. of IEEE Int'l Conf. on Electromechanical and Energy Systems* (SIELMEN'2023), Craiova – Chisinau, Romania – Moldova, Oct. 2023, 8 p.
25. Nevoloso, C.; Di Tommaso, A.O.; Miceli, R.; Scaglione, G.; Foti, S.; Testa, A. Impact analysis of FOC-based synchronous PWM strategy on traction induction motor drives performance. In: *Proc. of IEEE Int'l Conf. on Electrical Machines* (ICEM'2024), Torino, Italy, Sept. 2024, pp.1-7.

Citation: Oleschuk, V.; Vasiliev, I. Linear and non-linear voltage-to-frequency multi-zone control of synchronously modulated power electronic inverters. *Journal of Engineering Science*. 2025, XXXII (1), pp. 7-17. https://doi.org/10.52326/jss.utm.2025.8(2).01.

Submission of manuscripts: jes@meridian.utm.md